^{13}C and Deuterium Isotope Effects Suggest an Aldol Cleavage Mechanism for L-Ribulose-5-phosphate 4-Epimerase†

Lac V. Lee, Maria V. Vu, and W. W. Cleland*

Institute for Enzyme Research and Department of Biochemistry, University of Wisconsin, Madison, Wisconsin 53705

Received December 17, 1999

ABSTRACT: On the basis of ^{13}C and deuterium isotope effects, L-ribulose-5-phosphate 4-epimerase catalyzes the epimerization of L-ribulose 5-phosphate to D-xylulose 5-phosphate by an aldol cleavage to the enediolate of dihydroxyacetone and glycolaldehyde phosphate, followed by rotation of the aldehyde group and condensation to the epimer at C-4. With the wild-type enzyme, ^{13}C isotope effects were 1.85% at C-3 and 1.5% at C-4 at pH 7, with the values increasing to 2.53 and 2.05% at pH 5.5, respectively. H97N and Y229F mutants at pH 7 gave values of 3.25 and 2.53% at C-3 and 2.69 and 1.99% at C-4, respectively. Secondary deuterium isotope effects at C-3 were 2.5% at pH 7 and 3.1% at pH 5.5 with the wild-type enzyme, and 4.1% at pH 7 with H97N. At C-4, the corresponding values were 9.6, 14, and 19%. These data suggest that H97N shows no commitments, while the wild-type enzyme has an external commitment of ∼1.4 at pH 7 and an internal commitment independent of pH of ∼0.6. The Y229 mutant shows only the internal commitment of 0.6. The sequence of the epimerase is similar to those of L-fuculose-1-phosphate and L-rhamnulose-1-phosphate aldolases for residues in the active site of L-fuculose-1-phosphate aldolase, suggesting that Asp76, His95, His97, and His171 of the epimerase may be metal ion ligands, and Ser44, Gly45, Ser74, and Ser75 may form a phosphate binding pocket. The pH profile of *V*/*K* for L-ribulose 5-phosphate is bell-shaped with p*K* values of 5.94 and 8.24. The CD spectra of L-ribulose 5-phosphate and D-xylulose 5-phosphate differ sufficiently that the epimerization reaction can be followed at 300 nm.

L-Ribulose-5-phosphate 4-epimerase (araD, EC 5.1.3.4) catalyzes the interconversion of L-ribulose 5-phosphate (L-Ru5P)[1] and D-xylulose 5-phosphate (D-Xu5P) by changing the stereochemistry at C-4. The 4-epimerase is one of three

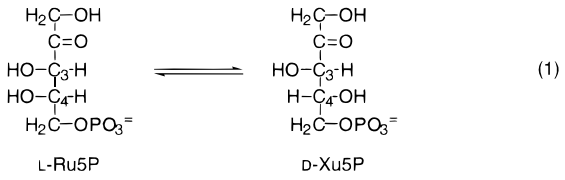

(1)

gene products of the arabinose operon (araBAD). By the concomitant processing of L-arabinose isomerase (araA), ribulokinase (araB), and the 4-epimerase (araD), the arabinose operon allows the prokaryote to convert L-arabinose into D-Xu5P, a pentose phosphate pathway intermediate (*1*). The entire operon, including the promotor region, has been cloned from *Eschericia coli* strain B/r (*2*). The enzyme has a molecular mass of 102 kDa and is believed to be composed of four identical 25.5 kDa subunits (*2*).

Epimerases can be divided into three groups on the basis of their catalytic mechanisms. In one group, the epimerization reaction occurs by abstraction of the acidic proton from a carbon α to the carbonyl group and redonation of it so as to change the chirality of the stereocenter (*3*−*6*). In the next group, catalysis occurs by an oxidation−reduction reaction involving hydride abstraction and donation about the carbon atom, usually a carbon atom *β* to the carbonyl group, with aid from a pyridine dinucleotide, NAD^+ or $NADP^+$. The epimerases that make use of redox chemistry all catalyze epimerization reactions on carbohydrates (*7*−*9*). A third group catalyzes mutarotation by breaking and reforming the C−O bond of the cyclic aldose with the resulting change in chirality at C-1 (*10*−*12*).

L-Ru5P 4-epimerase, however, appears to catalyze epimerization by a mechanism unrelated to the others. This 4-epimerase catalyzes the inversion of stereochemistry at the carbon *β* to the carbonyl group of L-Ru5P and D-Xu5P, but careful experiments have shown that catalysis occurs without the requirement of pyridine dinucleotides (*13*, *14*). It was also found that catalysis occurs with an absolute requirement for bivalent metal cations (*15*), without solvent exchange in the substrate or product (*14*, *16*), and without a sizable isotope effect for hydrogen transfer at C-4, the site of inversion of stereochemistry (*16*, *17*).

From these observations, Deupree and Wood (*15*) have proposed two possible mechanisms for the 4-epimerase-catalyzed epimerization reaction (Figure 1). The first mech-

† Supported by Grant GM 18938 from the National Institutes of Health.

* To whom correspondence should be addressed: 1710 University Ave., Madison, WI 53705. Phone: (608) 262-1373. Fax: (608) 265-2904. E-mail: cleland@enzyme.wisc.edu.

[1] Abbreviations: L-Ru5P, L-ribulose 5-phosphate; D-Xu5P, D-xylulose 5-phosphate; L-Fuc1P, L-fuculose 1-phosphate; L-Rhu1P, L-rhamnulose 1-phosphate; IRMS, isotope ratio mass spectrometer; ICPMS, inductively coupled plasma mass spectrometry.

10.1021/bi992894+ CCC: $19.00
Published on Web 03/29/2000

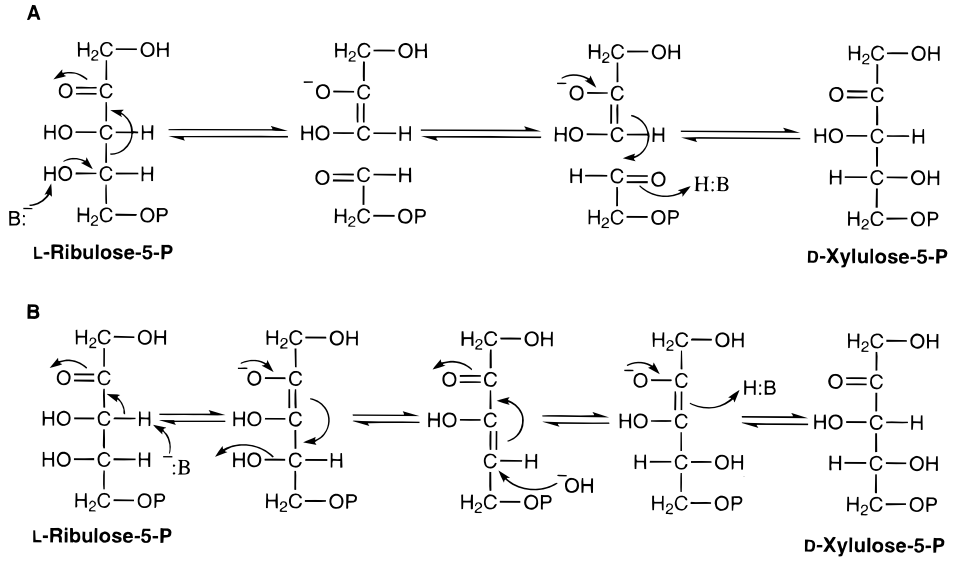

FIGURE 1: Mechanisms for L-Ru5P 4-epimerase catalyzed epimerization of L-Ru5P and D-Xu5P proposed by Deupree and Wood (*15*): (A) aldol cleavage−condensation mechanism and (B) dehydration−hydration mechanism.

anism (Figure 1A) involves the abstraction of the proton from the hydroxyl group on C-4, followed by cleavage of the bond between C-3 and C-4 to give a metal-stabilized dihydroxyacetone enediolate and a glycolaldehyde phosphate fragment. The C−C bond of glycolaldehyde phosphate is then rotated 180°, and the C−C bond between C-3 and C-4 is regenerated to give inversion of stereochemistry at C-4. The other proposed mechanism (Figure 1B) involves the abstraction of the proton at C-3 and formation of a metal-stabilized enediolate at C-2 and C-3, rearrangement of the double bond to C-3 and C-4 accompanying elimination of the hydroxyl group, and then the reverse process to give inversion at C-4. The first mechanism is analogous to the reaction catalyzed by a class II aldolase (*18*) where both aldol cleavage and condensation reactions occur, except that the 4-epimerase allows for racemization of the stereocenter at C-4. The second mechanism is analogous to one that is catalyzed by a dehydratase (*19*), where the complete dehydration−hydration cycle occurs with accompanying racemization at C-4.

The high degree of sequence alignment between L-Ru5P 4-epimerase and L-fuculose-1-phosphate (L-Fuc1P) aldolase has been noted by previous workers (*20*, *21*), and a similar alignment with L-rhamnulose-1-phosphate (L-Rhu1P) aldolase exists (Figure 2), which suggests that the 4-epimerase and the aldolases are evolutionally related. The crystal structure of the aldolase (*21*−*23*) indicates that four residues bind to the zinc(II) center in a configuration that was described as a distorted tetrahedral geometry. These four residues correspond to the Asp76, His95, His97, and His171 in the 4-epimerase. Mutants of three of these (H95N, H97N, and D76N) exhibit turnover numbers reduced by factors of 224, 3, and 140, respectively, with affinity for Zn^{2+} reduced to various degrees (*20*). We have mutated all of the tyrosines in the epimerase to phenylalanine and found the Y229F mutant to be more than 3 orders of magnitude slower than the wild-type 4-epimerase (*24*).[2]

The major thrust of this work involves measurement of ^{13}C and deuterium kinetic isotope effects on the epimerization reaction. The results show that the chemistry is partially rate-limiting for the wild-type enzyme and Y229F mutant, and almost entirely rate-limiting for the H97N mutant. They also show that the enzyme-catalyzed reaction occurs by an aldol cleavage−condensation mechanism (Figure 1A) and rule out the possibility that catalysis occurs by the dehydration−hydration mechanism (Figure 1B). These findings are in agreement with the recent report by Johnson and Tanner, who found that L-Ru5P 4-epimerase catalyzes a slow aldol condensation reaction between dihydroxyacetone and glycolaldehyde phosphate (*20*), a finding which suggested an aldol cleavage mechanism for the epimerase.

EXPERIMENTAL PROCEDURES

Materials and General Procedures. Lactate dehydrogenase was from Boehringer-Mannheim. Restriction enzymes, Deep Vent DNA Polymerase, and T4 DNA ligase were from New England Biolabs. Acetaldehyde, activated charcoal, dimethyl sulfoxide, glycolaldehyde, *n*-hexane, *n*-pentane, $MgCl_2$ (99.99% pure), and $ZnCl_2$ (99.999% pure) were from Aldrich. Sodium arsenate was from Mallinckrodt. IPTG was from U.S. Biochemical. All other biochemicals and enzymes were from Sigma. PTFE (0.45 μm) syringe filters (Nalge Co.) and Spectra/Por 4 Cellulose Dialysis Membranes (MW cutoff of 12000−14000) (Spectrum) were from Fisher Scientific. Dowex AG1X 8, AG50X8, and Chelex 100 were from Bio-Rad. Ultrafree-MC filters (MW cutoff of 10 kDa) were from Millipore.

Enzyme concentrations were determined according to the instructions of the Bio-Rad protein assay, which is based on the Bradford dye-binding procedure, with bovine serum albumin as the standard.

Overexpression and Purification of Ribulokinase (araB) and L-Ru5P 4-Epimerase (araD). The overexpression of both

[2] The structure of the *E. coli* epimerase has recently been determined to 2.4 Å resolution by X-ray crystallography and shows a fold very similar to that of the aldolase (N. Strynadka, personal communication). H95, H97, and H171 are metal ligands, while D76 is not; also, an ordered water is ligated in its place. Y229 could not be located, since the last eight C-terminal residues are disordered. The only tyrosine in the vicinity of the active site is Y141, but the Y141F mutant has full activity (*24*).

```
4-Ep  .......... .......... ........ML EDLKRQVLEA NLALPKHNLV  22
FucA  .......... .......... .......MER NKLARQIIDT CLEMTRLGLN  23
RhuA  MQNITQSWFV QGMIKATTDA WLKGWDERNG GNLTLRLDDA DIAPYHDNFH  50
      ---------- ---------- ---------- *-L---*-*- -*------*-

4-Ep  TLTW...GNV SAVDRERGVF VIKPSGVDYS IM...TADDM VVVSIETGEV  60
FucA  QGTA...GNV SV..RYQDGM LITPTGIPYE KL...TESH. .IVFIDGNGK  63
RhuA  QQPRYIPLSQ PMPLLANTPF IVTGSGKFFR NVQLDPAANL GIVKVDSDGA 100
      ---------- ---------* **-*G--*- -*------*- -*V-**--*-

4-Ep  .......VEG AKKPSSDTPT HRLLYQAFPS IGG.....IV HTHSRHATIW 104
FucA  .......HEE GKLPSSEWRF HMAAYQSRPD ANA.....VV HNHAVHCTAV 101
RhuA  GYHILWGLTN EAVPTSELPA HFLSHCERIK ATNGKDRVIM HCHATNLIAL 150
      ---------- *--*S*--- H--------- --------** H-H--*----

4-Ep  AQAGQSIPAT GTTHADYFYG TIPCTRKMTD AEINGEYEWE TGNVIVETFE 154
FucA  SILNRSIPAI HYMIAAAGGN SIPCAPYAT. ........FG TRELS....E 138
RhuA  TYVLENDTAV .FTRQLWEGS TECLVVFPDG VGILPWMVPG TDEIGQAT.. 197
      --------A- ---------- ---------- ---------* T-**------

4-Ep  KQGIDAAQMP GVLVHSHGPF AWGKNAEDAV ...HNAIVLE EVAYMGIFCR 201
FucA  HVALALKNRK ATLLQHHGLI ACEVNLEKAL WLAHEVEVLA QLYLTTLAIT 188
RhuA  ..AQEMQKHS LVLWPFHGVF GSGPTLDETF GLIDTAEKSA QVLVKVYSMG 245
      --*------- --L---HG-- *-*---*--- ---------- **--------

4-Ep  QLAPQLPDMQ QTLLNKHY.. ..LRKHGAKA YYGQ                  231
FucA  DPVPVLSDEE IAVVLEKFKT YGLRIEE... ....                  215
RhuA  GMKQTISREE LIALGKRFGV TPLASALAL. ....                  274
      -----*---* ---*--**-- --L------- ----
```

FIGURE 2: Sequence alignments of L-Ru5P 4-epimerase, L-Fuc1P aldolase, and L-Rhu1P aldolase. The X-ray crystal structure of L-Fuc1P aldolase shows that residues Glu73, His92, His94, and His155 (in solid boxes) are zinc ligands (*21*−*23*). Residues Thr43, Gly44, Ser71, and Ser73 (in dotted boxes) constitute the binding pocket for the phosphate group of the substrate (*21*−*23*). The alignment suggests that residues Asp76, His95, His97, and His171 of L-Ru5P 4-epimerase may be metal ion ligands and that Ser44, Gly45, Ser74, and Ser75 may bind the phosphate group of the substrate, since these groups are conserved in all three enzymes. The recently determined X-ray structure shows that the histidines are metal ion ligands, while Asp76 is not (N. Strynadka, personal communication).

ribulokinase and the 4-epimerase first involved the subcloning of the araB and araD genes into pET expression vectors (Novagen). The araB and araD genes were amplified by PCR from the pNL16 plasmid that contains the entire araBAD operon [a gift from N. Lee of the University of California at Santa Barbara, Santa Barbara, CA (*3*)]. The newly constructed plasmids were transformed separately into BL21-(DE3)pLysS *E. coli* strain B (Novagen). The cells were grown in LB medium and induced with IPTG for overexpression of the enzymes. The purification of the ribulokinase and 4-epimerase were carried out according to published methods (*25*, *26*), which involved ammonium sulfate precipitation of the enzymes and column chromatography (anion exchange and gel filtration). A detailed description of the procedure outlined above is in the Supporting Information.

Preparation of Mutant Plasmids and Enzymes. The mutant plasmids for the expression of Y229F and H97N mutant 4-epimerases were generated using the QuikChange Site-Directed Mutagenesis Kit from Stratagene (*24*). The plasmids were transformed into B(DE3)araD$^-$ cells for overexpression of the enzymes (*24*). The mutant enzymes were purified in the same manner as the wild-type enzyme.

Preparation of Zinc-Substituted 4-Epimerase and Metal Content Analysis. L-Ru5P 4-epimerase purified from the overexpression system was determined by ICPMS to contain 98.4% zinc, along with 1.33% manganese and 0.22% cobalt. The ICPMS analysis showed that there was 0.87 equiv of metals per subunit of enzyme, in relatively good agreement with the 1.05 value previously reported (*20*). The apoenzyme of the wild-type 4-epimerase and the Y229F mutant was generated by dialyzing the column-purified 4-epimerase in 250 mL of 20 mM EDTA and 1 mM DTT (pH 7.0) for 3−4 h at room temperature, followed by three additional cycles of 250 mL of 10 mM KHEPES (pH 7.0) and 100 mM KCl, and two additional cycles of 250 mL of 10 mM KHEPES (pH 7.0). These buffer solutions were freed of metal ions by passing the solutions through a column of Chelex 100 resin. Finally, the enzyme was passed through an EDTA-treated Pharmacia PD-10 gel filtration column that was pre-equilibrated with 10 mM KHEPES (pH 7.0) to remove any remaining salts and EDTA. The wild-type 4-epimerase and the Y229F mutant were reconstituted with 2 equiv of $ZnCl_2$ per active site.

The apoenzyme of the H97N mutant was generated by a single passing the purified enzyme through a small Chelex 100 column (4 cm length, 2 mL volume) equilibrated in 10 mM KHEPES (pH 7.0) buffer. The H97N mutant was also reconstituted with 2 equiv of $ZnCl_2$ per active site. All analyses of metal content were carried out by ICPMS at the University of Wisconsin Soil and Plant Analysis Laboratory.

Synthesis of L-Ru5P (27). Twenty-five grams of L-arabinose was refluxed under dry conditions in 200 mL of

distilled pyridine for 5 h. Pyridine was removed by evaporation, and unreacted L-arabinose was removed by precipitation with ethanol. The ^{1}H NMR spectrum of the crude L-ribulose showed traces of pyridine, which was removed by extraction with methylene chloride. The crude L-ribulose, which was light caramel in color, was clarified by treatment with activated charcoal (yield of 2.5 g).

For synthesis of L-Ru5P, the reaction mixture contained 40 mM L-ribulose (10 mmol), 0.76 mM ATP, 13 mM $MgCl_2$, 31.7 mM acetyl phosphate (7.9 mmol), 196 units of ribulokinase, and 270 units of acetate kinase in 250 mL, with the limiting reagent being the acetyl phosphate. As the reaction proceeded, the pH required periodic readjustment to 7.6 with 1 M KOH. After 1.5 h, the pH of the solution ceased changing, indicating that the reaction was finished. Use of acetyl phosphate and acetate kinase to recycle the ADP allowed the use of low levels of ATP, which facilitated its removal after the reaction by treatment with activated charcoal. The enzymes were removed by filtration through a PM10 (MW cutoff of 10 kDa) Diaflo Ultrafiltration Membrane (Amicon Inc.). Once the ADP/ATP and enzymes were removed, a slight molar excess of solid barium chloride (11 mmol) was added to the solution and 4 volumes of absolute ethanol was added to precipitate barium L-Ru5P, which was collected by centrifugation and dried by lyophilization. The barium was exchanged for protons by passing the redissolved salt through a column of Dowex AG50X8 (H^+ form). The pH of the eluted L-Ru5P was adjusted to 7.0 with 1 M NaOH, and the sodium salt of L-Ru5P was then stored frozen in small aliquots (yield of 90%). The ^{1}H NMR spectrum of the L-Ru5P sample indicated it was free of carbohydrate impurities.

Epimerization Assay Conditions and the pH Profile. The epimerization reaction in the L-Ru5P to D-Xu5P direction was assayed at 22 °C (*16*). The components of the assay were 50 mM buffer (K^+ form), 10 mM $MgCl_2$, 0.2 mM NADH, 5 mM D-ribose 5-phosphate, 0.1 mM TPP, 1 unit of transketolase, 50 units of triosephosphate isomerase, 10 units of α-glycerophosphate dehydrogenase, 0.1 unit of L-Ru5P 4-epimerase, and varying concentrations of L-Ru5P. The reaction was started by the addition of the 4-epimerase and followed by the decrease in absorbance of NADH at 340 nm ($\epsilon_{340} = 6.22$ mM^{-1} cm^{-1}). The buffers were MES (pH 5.5−6.5), HEPES (pH 7.0−8.0), and CHES (pH 8.5). The L-Ru5P concentrations were kept between 0.01 and 5 mM to encompass the shift in K_m values of L-Ru5P as the pH was varied.

Initial velocities were fitted to eq 2 to obtain the V_{max} and K_m values for the epimerization reaction. The V/K pH profile was generated by fitting the data to eq 3. Fitting was done with the FORTRAN programs of Cleland (*28*).

$$v = \frac{VA}{K + A} \tag{2}$$

$$\log Y = \log\left(\frac{C}{1 + \frac{H}{K_a} + \frac{K_b}{H}}\right) \tag{3}$$

Determination of ^{13}C Kinetic Isotope Effects. Measurement of ^{13}C kinetic isotope effects was achieved by the internal competition method, using the natural abundance of ^{13}C as the trace label (*29*). The isotopic ratios were determined with a Finnigan MAT Delta isotope ratio mass spectrometer (IRMS). Kinetic isotope effects were calculated using the isotopic ratios of a specific carbon from the product (R_p) or residual substrate (R_s) from a partial conversion reaction and the isotopic ratio from the same carbon in the starting material (R_o). R_o was determined by complete conversion of the substrate to product. Equation 4 was used to calculate the observed isotope effect from the isotopic ratios of the product and starting material at a known fractional conversion, *f*, of the reaction. Equation 5 was used to calculate the isotope effect from the isotopic ratios of the residual substrate and starting material.

$$^{13}(V/K) = \frac{\log(1 - f)}{\log[1 - f(R_p/R_o)]} \tag{4}$$

$$^{13}(V/K) = \frac{\log(1 - f)}{\log[(1 - f)(R_s/R_o)]} \tag{5}$$

The kinetic isotope effect measurements required the use of coupling enzymes to remove the product, since the epimerization reaction is reversible. After the 4-epimerase had converted L-Ru5P to D-Xu5P, transketolase transferred C-1 and C-2 of D-Xu5P to glycolaldehyde to form L-erythrulose and D-glyceraldehyde 3-phosphate (*30*). With arsenate and NAD^+, D-glyceraldehyde 3-phosphate was converted to 3-PGA by D-glyceraldehyde-3-phosphate dehydrogenase. NADH was recycled back to NAD^+ with acetaldehyde and alcohol dehydrogenase. Therefore, C-3−C-5 of L-Ru5P became C-1−C-3 of 3-PGA, respectively (see below for experimental details).

Once L-Ru5P and 3-PGA were purified (see below for details), L-Ru5P and glycerate (from 3-PGA by treatment with alkaline phosphatase) were treated with $NaIO_4$. The periodate degradation resulted in the production of CO_2 from C-2 of L-Ru5P and CO_2, formate, and formaldehyde from C-1−C-3, respectively, of glycerate. The CO_2 samples were analyzed on the IRMS. Formate was converted to CO_2 by I_2 oxidation for isotope ratio analysis, and the carbon isotope ratio of formaldehyde was acquired indirectly by calculation (see below). These procedures allowed for the measurement of the isotope ratios of C-2−C-5 of L-Ru5P.

At least three reactions were performed for the complete and partial conversion reactions to acquire a complete set of carbon isotope effect data at each pH for each enzyme. The conditions for the complete conversion reaction were 10 mM sodium arsenate (pH 7.0), 1 mM $MgCl_2$, 0.1 mM $ZnCl_2$, 0.4 mM NAD^+, 2 mM L-Ru5P, 50 mM glycolaldehyde, 0.1 mM TPP, 15 mM acetaldehyde, 0.1 unit/mL Zn(II)-substituted L-Ru5P 4-epimerase, 0.5 unit/mL transketolase, 25 units/mL D-glyceraldehyde-3-phosphate dehydrogenase, and 50 units/mL alcohol dehydrogenase. The activity ratio (in units) for 4-epimerase, transketolase, glyceraldehyde-3-phosphate dehydrogenase, and alcohol dehydrogenase was thus 1:5:250:500. This reaction was allowed to occur for 8 h at room temperature. The conditions for partial conversion were similar to those of the complete conversion reaction except that 1 mM sodium arsenate (pH 5.5 or 7.0), 4 mM L-Ru5P, and 0.01 unit/mL L-Ru5P 4-epimerase were used. The activity ratio was then 1:50:2500:5000. Partial conversion reactions were allowed to reach a fractional conversion

of 0.25−0.35. All necessary cofactors were at concentrations well above K_m levels. Both complete and partial conversion reactions were carried out in a volume of 50 mL. The pH decreased as the reaction proceeded, and adjustments were made with 1 M NaOH to keep the pH at ±0.05 of the desired level. The reactions were started by the addition of the 4-epimerase.

The extent that L-Ru5P was converted to D-Xu5P by the 4-epimerase and converted to 3-PGA by the coupling enzymes was determined periodically by assaying for 3-PGA. A 200 μL aliquot of the conversion reaction mixture was first filtered free of enzymes by centrifugation with a Millipore Ultrafree-MC filter (MW cutoff of 10 kDa), and 3-PGA was assayed with 50 mM HEPES, 10 mM $MgCl_2$, 3 mM ADP, 0.2 mM NADH, 1 mM 2,3-diphosphoglycerate, 3 units/mL phosphoglyceromutase, 3 units/mL enolase, 3 units/mL pyruvate kinase, and 5 units/mL lactate dehydrogenase. The reaction was followed by the decrease in absorbance of NADH at 340 nm. The reaction was also monitored by assaying for residual L-Ru5P by the continuous assay (above), and the results from both assays produced very similar values.

At the desired fractional conversion, the solution was quickly adjusted to pH 4 to halt the reaction and the solution was passed through the Amicon PM10 filter. The fractional conversion was determined again to obtain the final value. NAD^+, NADH, and TPP were then removed from the reaction mixture by passing it through a 1.5 cm × 3.5 cm column of activated charcoal. Three passes were required to remove all of the aromatic compounds (monitored by the change at A_{260}). The charcoal fines introduced into the sample were removed by filtering the solution through a sterile 0.45 μm pore PTFE syringe filter (Nalge Co.).

The volume of the reaction solution was adjusted to 150 mL, and the pH was readjusted to 7.0 with 5 M NaOH. The solution was loaded onto a 2.5 cm × 30 cm column of Dowex AG1X8-Cl^- (100−200 mesh), which was washed with 1000 mL of distilled water to elute all noncharged molecules (glycolaldehyde, acetaldehyde, L-erythrulose, and ethanol). Residual L-Ru5P and 3-PGA were eluted with a 2000 mL linear gradient of 0 to 100 mM HCl. The fractions containing L-Ru5P and three-quarters of the pooled 3-PGA fractions were saved for the periodate degradation reaction (see below). The remaining quarter of the 3-PGA material was evaporated to a small volume (0.5 mL) and transferred to a quartz tube, 25 cm × 0.7 cm and 2 mm thick. The residual H_2O was removed by aspiration, and CuO (10 g) and silver metal (0.2 g) were added to the quartz tube. The tube was placed on the vacuum line, sealed, and heated to 750 °C for 2 h to combust the 3-PGA. After the combustion, the tubes were cracked on the vacuum line and the resulting CO_2 was distilled through two dry ice/isopropyl alcohol traps (−80 °C) to remove H_2O and collected in a liquid nitrogen trap. The collected gas, which consists of the three one-carbon fragments from 3-PGA, was then analyzed with the IRMS. The measured carbon isotope ratio (^{13}C:^{12}C) of combusted 3-PGA is therefore the average of the isotope ratios of the individual carbons:

$$R_{3-PGA} = \frac{R_{C-1} + R_{C-2} + R_{C-3}}{3} \qquad (6)$$

The saved portions of purified L-Ru5P and 3-PGA, each about 50 μmol after the workup, were transferred to separate 100 mL round-bottom flasks and dried on the rotoevaporator (25 °C water bath for L-Ru5P and 30 °C water bath for 3-PGA) for 1 h to remove both water and as much HCl as possible. For the 3-PGA sample only, 25 mL of distilled water, 0.5 mL of 250 mM CHES, pH 9.5 buffer (pH adjusted with saturated NaOH solution), and 0.125 mL of 200 mM $MgCl_2$ were added to the flask. One to two milligrams of bovine alkaline phosphatase (50 units/mg) was added to dephosphorylate the 3-PGA. After dephosphorylation for 5 h at 37 °C, the reaction mixture was passed through a PM10 membrane filter to remove the alkaline phosphatase. The solution was adjusted to pH 7.0 with 1 M HCl, and the sample was transferred to a sealable flask with a sidearm containing a stir bar. The L-Ru5P sample (25 mL) was also transferred to a flask with a sidearm and a stir bar, and the pH was adjusted to 7.0 with saturated NaOH. Both samples were sparged with CO_2-free N_2 gas for 8 h, and the stopcocks were then closed. Sparged 250 mM $NaIO_4$ (0.6 mL) was injected through the sidearm into the glycerate flask, while 1 mL of the $NaIO_4$ solution was injected into the L-Ru5P flask. Degradation of glycerate was allowed to occur for 4 h at room temperature, while degradation of L-Ru5P was allowed to occur for 5 h at 37 °C (*31*).

L-Ru5P was cleaved into formaldehyde, CO_2, formate, and glycolaldehyde phosphate from C-1, C-2, C-3, and C-4/C-5, respectively. The CO_2 was isolated by first connecting the flask with the reacted L-Ru5P to the vacuum line. The flask was frozen in liquid N_2, and the N_2 gas that was introduced during the sparging process was evacuated. The flask was then warmed with room-temperature water until the contents were melted and then refrozen in a dry ice/isopropyl alcohol bath. The CO_2 was distilled through two dry ice/isopropyl alcohol traps and into a liquid nitrogen trap. The flask was then thawed, frozen, and distilled three additional times. The collected CO_2 was analyzed with the IRMS to determine the isotopic ratio at C-2 of L-Ru5P. The other carbon species from L-Ru5P were discarded.

For the partial conversion reactions, the carbon isotope ratio of the CO_2 from C-2 of L-Ru5P represented the R_s value. To obtain the R_o value at C-2, L-Ru5P from the stock solution was reacted with periodate to liberate C-2 as CO_2 and isolated as described above. Since the fractional conversion for the reaction had been previously determined, eq 3 was used to calculate the ^{13}C isotope effect at C-2.

The CO_2 from the flask containing the reacted glycerate was isolated the same way as the CO_2 from L-Ru5P and analyzed on the IRMS to acquire the isotopic ratio at C-1 of glycerate (derived from C-3 of L-Ru5P). After four freeze−distill−thaw cycles to isolate C-1 of glycerate, the volatile material that was trapped in the dry ice/isopropyl alcohol traps was recondensed back into the flask, with liquid N_2 beneath the flask, to ensure that no formic acid (derived from C-2 of glycerate or C-4 of L-Ru5P) would be lost. The condensation was allowed to occur for 30 min; the sample was thawed, and the pressure inside the flask was re-equilibrated to atmospheric pressure with a balloon filled with CO_2-free N_2 gas. Saturated NaOH (20 μL) was injected into the flask to raise the pH to about 10. The sample was stirred for 30 min to ensure that all of the formic acid was

in solution. It was then removed from the sealed flask, and the pH was adjusted to below 1.0 with analytical grade concentrated sulfuric acid.

The formic acid was then purified by azeotropic distillation at 61 °C from 700 mL of pure *n*-hexane. The source flask containing the formic acid was stirred vigorously with a stir bar since it was found that the transport of formic acid from the aqueous layer to the hexane layer was a slow process. Also, the variac was set for slow distillation to allow adequate time for the formic acid to be transported between layers. The receiving flask contained approximately 40 mL of distilled water and 1 drop of saturated NaOH solution so that the formic acid from the azeotropic formic acid/hexane mixture could be captured. Vigorous stirring of the solution with a stir bar in the receiving flask during the distillation was also employed to ensure maximum recovery of the formic acid.

The aqueous (bottom) layer of the receiving flask was transferred into a separate flask, and 1 mL of 1 M NaHEPES (pH 7.5) (made with saturated NaOH) was added. The solution was then sparged for 12 h. Next, the solution was concentrated to approximately 0.5 mL by rotoevaporation, and the sample was transferred to a sealable flask with a sidearm and a stir bar. The rest of the H_2O from the sample was removed on the vacuum line with stirring, and the resulting salt pellet was further dried for 3 h at 70 °C in a vacuum. After 3 h, the small pocket of air in the sidearm was flushed twice with CO_2-free N_2 gas from a balloon. The flushing of the sidearm was carried out to minimize CO_2 contamination of the sample during the period when the I_2 solution was injected into the flask. The pressure inside the flask was equilibrated to atmospheric pressure with N_2 gas from a balloon, and a solution of 0.3 g of I_2 in 2 mL of anhydrous DMSO was injected into the flask. The sample in the flask was quickly frozen with liquid N_2, and the gaseous N_2 was evacuated from the flask. Any CO_2 that was immediately formed from I_2 oxidation of formate was collected in the liquid N_2 trap with two previous *n*-pentane/liquid N_2 traps used for trapping the less volatile DMSO. The temperature of the *n*-pentane/liquid N_2 traps was kept between −120 to −128 °C. The sample was then thawed to room temperature to allow the oxidation reaction to proceed to completion. The oxidation of formate and the distillation of CO_2 were allowed to occur for 1 h, with stirring, to ensure that all the CO_2 was collected. The CO_2 was analyzed with the IRMS to determine the isotopic ratio of C-2 of glycerate (derived from C-4 of L-Ru5P).

The quantitative conversion of formaldehyde (from C-3 of glycerate) to CO_2 is difficult since formaldehyde has a significant vapor pressure and also a tendency to polymerize in concentrated solutions. Acquiring the isotope ratio for formaldehyde was therefore done indirectly. The carbon isotope ratio for 3-PGA (the precursor to glycerate) had been determined previously. The isotope ratios for C-1 and C-2 for glycerate were measured. Therefore, using eq 6, the isotopic ratio at C-3 (R_{C-3}) could be calculated. The isotopic ratios for C-1−C-3 of glycerate (from C-3−C-5 of L-Ru5P, respectively) from the partial conversion reaction (R_p), along with the isotope ratios from the complete conversion reaction (R_o) acquired in the same manner, allowed for the calculation of carbon kinetic isotope effects via eq 4. Altogether, the ^{13}C kinetic isotope effects at C-2−C-5 of L-Ru5P were determined.

As a control experiment, the coupling enzymes for the partial conversion reaction were doubled to test if the epimerization reaction is indeed the rate-limiting step in the series of reactions which culminated in the conversion of L-Ru5P to 3-PGA. The ^{13}C kinetic isotope effects were measured as stated above and found to be the same as those measured under "normal" conditions.

Circular Dichroism Spectra of L-Ru5P and D-Xu5P. The CD spectra of L-Ru5P and D-Xu5P were taken with the Aviv CD model 62A DS spectrometer with the temperature being set at 25 °C. The solution that was measured contained 8 mM L-Ru5P or D-Xu5P in 50 mM KHEPES (pH 7.0) or 50 mM potassium acetate (pH 5.5). Blanks with corresponding buffers but no carbohydrates were also taken and their spectra subtracted from the spectra containing the carbohydrates.

The millimolar ellipticities at 300 nm used in measuring rates in the equilibrium perturbation experiments were 11.69° at pH 7.0 and 8.877° at pH 5.5 for L-Ru5P and 0.9700° at pH 7.0 and 0.6892° at pH 5.5 for D-Xu5P.

Synthesis of D-[3-^{2}H]Xu5P and D-[4-^{2}H]Xu5P. The synthesis of D-Xu5P deuterated at C-3 was carried out in two steps. The first reaction mixture contained 50 mM D-ribose 5-phosphate, 1000 units of phosphoriboisomerase, and 100 units of D-ribulose-5-phosphate 3-epimerase at pD 7.5 in 300 mL of D_2O. After 8.5 h, the reaction produced equilibrium concentrations of D-ribose 5-phosphate, D-ribulose 5-phosphate, and D-Xu5P with deuterium incorporated at C-1 and C-3 of D-Xu5P. The enzymes were removed with an Amicon PM10 filter. In the second step, 36.7 mM acetyl phosphate, 4.5 mM ATP, 500 units of phosphoriboisomerase, 250 units of phosphoribulokinase, 500 units of acetate kinase, and 4 mM $MgCl_2$ were added to the reaction mixture. This converted both D-ribose 5-phosphate and D-ribulose 5-phosphate to D-ribulose 1,5-diphosphate, leaving deuterated D-Xu5P untouched. The pH required periodic readjustment to pD 7.5 with 1 M KOD during the course of the reaction. Once the pH had ceased changing, the reaction mixture was allowed to sit for 0.5 h and the enzymes were filtered off.

The reaction mixture was then loaded onto a 2.5 cm × 30 cm column of Dowex AG1X8-Cl^-. Deuterated D-Xu5P and D-ribulose 1,5-diphosphate were separated by a 2000 mL linear gradient from 0 to 100 mM HCl. The fractions containing deuterated D-Xu5P, detected by the coupled enzyme assay without the 4-epimerase present, were pooled, and the pH was adjusted to 7.0 with $Ba(OH)_2$. Four volumes of absolute ethanol was added to precipitate the barium salt of deuterated D-Xu5P. The precipitated sugar was collected by centrifugation, and the residual ethanol was removed by lyophilization. The barium D-Xu5P was dissolved in H_2O, and the barium was exchanged for protons by passing the solution through a column of Dowex 50WX8-H^+. The pH was readjusted with 1 M NaOH to 7.0, and the sample was concentrated by rotoevaporation and stored in small aliquots at −80 °C.

The ^1H NMR data of the deuterated D-Xu5P indicated that there was 65% deuterium incorporation at C-1 (a position that should not cause an isotope effect) and 100% incorporation at C-3. Also, there was some D-ribose 5-phosphate contamination. However, this impurity did not affect the

measurement of deuterium isotope effects by equilibrium perturbation.

The synthesis of D-[4-^{2}H]Xu5P required large quantities of dihydroxyacetone phosphate. Although it is available commercially, its high cost led us to synthesize this starting material. The reaction mixture contained 100 mM dihydroxyacetone, 50 mM acetyl phosphate (sodium form), 0.3 mM ATP, 2000 units of glycerokinase, 500 units of acetate kinase, and 4 mM $MgCl_2$ in a volume of 600 mL (*32*). The pH of the solution was 8.5 and adjusted with 1 M NaOH. As the reaction proceeded, periodic additions of NaOH were needed to hold the pH constant. The reaction was completed within 2 h, as indicated by the lack of change in pH. The enzymes were then removed with the Amicon PM10 filter. The pH was readjusted to 7.0 with 1 M HCl, and solid barium chloride was added for a total concentration of 55 mM. Some precipitate observed immediately was removed by centrifugation. Four volumes of absolute ethanol was then added to precipitate dihydroxyacetone phosphate, which was collected by centrifugation.

The barium salt of dihydroxyacetone phosphate was dissolved in water and the barium exchanged for H^+ with Dowex 50WX8-H^+, and the pH was readjusted to 7.0 with 1 M NaOH. The solution was concentrated to a small volume by rotoevaporation (bath at 25 °C), and the rest of the H_2O was removed by lyophilization. Once dried, the dihydroxyacetone phosphate was redissolved in D_2O to a final concentration of 50 mM.

To 100 mL of 50 mM dihydroxyacetone phosphate in D_2O was added 500 units of triosephosphate isomerase. The reaction was allowed to occur until the H_R proton on C-1 of dihydroxyacetone phosphate and the C-2 proton of glyceraldehyde 3-phosphate had exchanged with the D_2O solvent, as determined by ^{1}H NMR [triosephosphate isomerase does not exchange the H_S proton with solvent (*33*)]. Additional dry reagents and enzyme were added to give final concentrations of 150 mM hydroxypyruvate, 0.1 mM TPP, 200 units of transketolase, and 10 mM $MgCl_2$ (anhydrous). Transketolase catalyzes the addition reaction between hydroxypyruvate and glyceraldehyde 3-phosphate to give D-Xu5P and CO_2 (*30*). The reaction was allowed to occur for 12 h to about 90% completion, as determined by the assay for residual dihydroxyacetone phosphate (10 units of α-glycerophosphate dehydrogenase and 0.2 mM NADH). If the reaction were allowed to occur for too long, polymerization of the carbohydrates was observed, as indicated by the yellowing of the reaction solution. The enzymes were then removed with an Amicon PM10 filter.

The residual dihydroxyacetone phosphate was converted to fructose 1,6-bisphosphate with the addition of 3 mg each of triosephosphate isomerase and aldolase. This reaction was allowed to proceed for about 2 h until most of the dihydroxyacetone phosphate was consumed. The enzymes were removed by filtration.

Before purification of the D-[4-^{2}H]Xu5P, TPP was removed with activated charcoal. The D-[4-^{2}H]Xu5P was purified on a 2.5 cm × 30 cm column of Dowex AG1X8-Cl^-. The phosphorylated sugars were eluted with 2000 mL of a linear gradient from 0 to 100 M HCl. The fractions containing D-[4-^{2}H]Xu5P were located with the assay for D-Xu5P, pooled, and adjusted to pH 7.0 with a solution of saturated $Ba(OH)_2$. Four volumes of absolute ethanol was added to the solution to precipitate the barium salt of deuterated D-Xu5P. This was converted to the sodium salt as was done for the other compounds described above and was concentrated by rotoevaporation and stored in small aliquots at −80 °C. The ^{1}H NMR spectrum of D-[4-^{2}H]Xu5P showed that deuterium incorporation was 100% at C-4 and 0% at C-3. About 46% deuterium incorporation was observed at C-1, a position not expected to cause an isotope effect.

Determination of Deuterium Kinetic Isotope Effects by Equilibrium Perturbation. In the equilibrium perturbation method, enzyme is added to a labeled substrate and unlabeled product at equilibrium (*34*, *35*). The unlabeled product reacts faster than the labeled substrate, causing a perturbation from equilibrium, but as isotopic mixing takes place, the reaction returns to the equilibrium position. The size of the perturbation permits calculation of the isotope effect.

To measure the kinetic isotope effects without interference from heavy metal contamination, care was taken to remove all heavy metal ions from substrates and buffer solutions by passing the solutions through Chelex 100 columns. The wild-type 4-epimerase and the H97N mutant were also stripped of any heavy metals either by dialysis with EDTA (wild-type) or by Chelex 100 (H97N) treatment and reconstituted with a 1:2 ratio of enzyme to $ZnCl_2$ (above).

Measurement of secondary deuterium isotope effects by the equilibrium perturbation method was achieved by the "one-pot" method (*34*). Once the light and heavy species were mixed to equilibrium concentrations (K_{eq} = 1.90 favoring D-Xu5P;[3] in this case, the L-Ru5P/D-[3-^{2}H]Xu5P and L-Ru5P/D-[4-^{2}H]Xu5P mixtures), the same pot was used to measure the isotope effects for both the wild-type enzyme and the H97N mutant.

After the substrates were made metal ion-free with Chelex 100, the concentrations of the substrates were measured carefully by enzymatic end-point assay (above). The light and heavy species were then mixed to equilibrium concentrations. Some additional adjustments of the light and heavy mixture were needed because the initial perturbations did not approach baseline. Successive titration of the one-pot mixture with small quantities of the required substrate eventually allowed the perturbation to reach baseline. This trial and error process was carried out at pH 7 with the wild-type enzyme. Once the light/heavy mixtures reached equilibrium concentrations, the equilibrium perturbation was then assessed by addition of wild-type enzyme or the H97N mutant at pH 7.0. Next, the pH of this pot was readjusted from pH 7.0 to 5.5, and the perturbation was assessed with the wild-type enzyme. The perturbation was not assessed for the Y229F mutant because its catalytic activity was too slow to allow for the measurement of the perturbation (*24*).

For the L-Ru5P/D-[3-^{2}H]Xu5P mixture, the L-Ru5P concentration was 8.79 mM and the D-[3-^{2}H]Xu5P concentration was 16.7 mM. For the L-Ru5P/D-[4-^{2}H]Xu5P mixture, the L-Ru5P concentration was 4.86 mM and the D-[4-^{2}H]Xu5P concentration was 9.23 mM. Higher concentrations were used for the L-Ru5P/D-[3-^{2}H]Xu5P mixture because the extent of

[3] A K_{eq} of 1.90 was measured by end point assays, while a value of 1.20 was observed by proton NMR integration. The value of 1.9 is the correct one, since this was the product-to-substrate ratio required in equilibrium perturbation experiments for the reaction to return to the starting point.

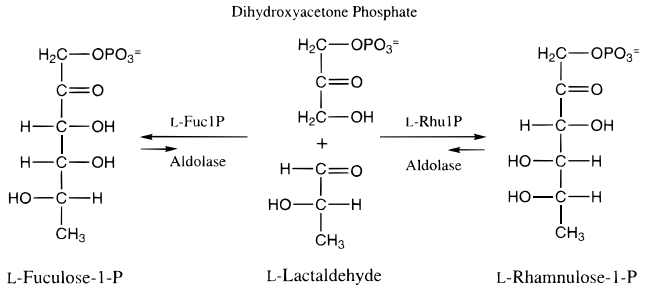

FIGURE 3: Catalyzed reactions of class II L-Fuc1P aldolase and L-Rhu1P aldolase. Both aldolases share common substrates, dihydroxyacetone phosphate and L-lactaldehyde. The addition products are different only in the stereochemistry at C-4.

the observed perturbation was smaller than that of the L-Ru5P/D-[4-^{2}H]Xu5P mixture. Each mixture also contained 0.1 mM $ZnCl_2$ in 50 mM KHEPES (pH 7.0) or 50 mM potassium acetate (pH 5.5). The reaction was started by the addition of the wild type or the H97N mutant. The change in ellipticity was measured at 300 nm in a 1 cm, 1 mL quartz cuvette.

The equilibrium perturbation measurement with D-[4-^{2}H]-Xu5P was carried out on the Jasco-41C CD spectrometer, while the measurement with D-[3-^{2}H]Xu5P was carried out with the Aviv CD model 62A DS spectrometer because of its greater sensitivity. Both instruments were calibrated with D-camphor ($\epsilon_{285} = 0.1486$ mL mg^{-1} and $\theta_{290.5} = 355°$ mL mg^{-1} cm^{-1}).

The calculation of the kinetic isotope effects from the measured equilibrium perturbations was done using eqs 7 and 8 (*34*, *35*).

$$\frac{A_{max} - A_o}{A_o'} = \alpha^{-1/(\alpha - 1)} - \alpha^{-\alpha/(\alpha - 1)} \quad (7)$$

$$A_o' = \frac{1}{1/A_o + 1/P_o} \quad (8)$$

A_o and P_o are the initial L-Ru5P and deuterated D-Xu5P concentrations at equilibrium. $(A_{max} - A_o)/A_o'$ represents the size of the perturbation measured on the CD spectrometer, and α is the calculated deuterium isotope effect. These equations are simpler than those usually used for this method (*34*, *35*) because the equilibrium isotope effects for the epimerization reaction are unity.

RESULTS

Sequence Alignment. Previous workers have shown that the sequence of L-Ru5P 4-epimerase is similar to that of L-Fuc1P aldolase in that groups in the active site of the latter are highly conserved (*20*, *21*, *36*). A search in the GCG database (*37*) for sequence similarity between the 4-epimerase and aldolases or dehydratases showed that L-Rhu1P aldolase (*38*) also is similar to L-Fuc1P aldolase. A match was not found with the 4-epimerase unless all three enzymes were compared together, in which case the groups in the active site of L-Fuc1P aldolase are conserved (Figure 2).

The reactions catalyzed by L-Fuc1P and L-Rhu1P aldolases are shown in Figure 3. These aldolases cleave six carbon sugars phosphorylated at C-1, while L-Ru5P 4-epimerase cleaves a five-carbon sugar phosphorylated at C-5 during its reaction. The substrates for the aldolases are thus inverted

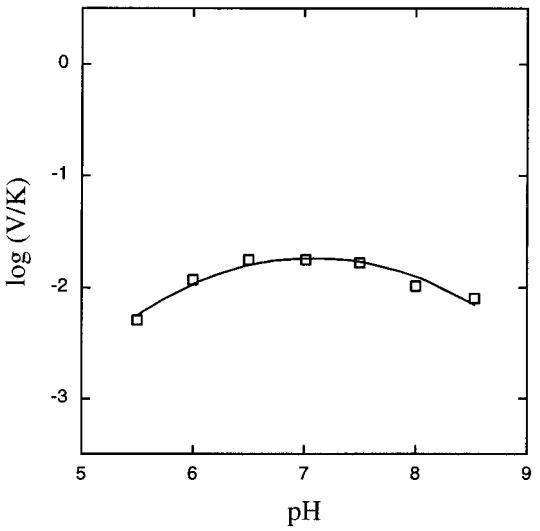

FIGURE 4: *V*/*K* vs pH profile of wild-type L-Ru5P 4-epimerase. The p*K* values from a fit to eq 3 were 5.94 ± 0.12 and 8.24 ± 0.14. See Experimental Procedures for assay conditions.

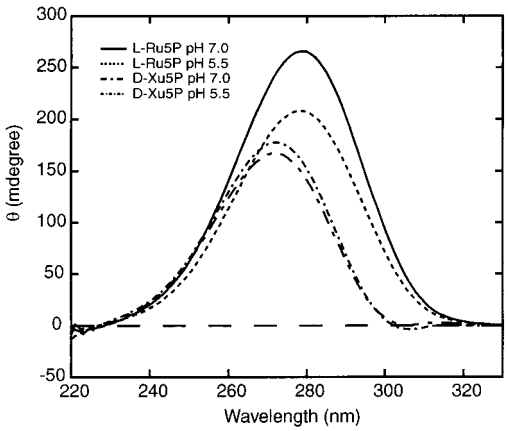

FIGURE 5: CD spectra of L-Ru5P and D-Xu5P. See Experimental Procedures for the conditions of data collection.

in the active site relative to the positioning in the epimerase site. The metal ion-bound enediolate of dihydroxyacetone is phosphorylated in the aldolase reactions, which is not so for the epimerase.

pH Profile. The *V*/*K* versus pH profile of the 4-epimerase (Figure 4) was bell-shaped with the maximum near pH 7.0 and the *V*/*K* values decreasing toward the acidic or basic regions with p*K* values of 5.94 and 8.24. Values below pH 5.5 or above pH 8.5 were difficult to obtain since the coupling enzymes in the continuous assay showed a significant decrease in activity in those regions. The *V*/*K* profile was used to determine the pH regions to use for measurement of the kinetic isotope effects.

CD Spectra of L-Ru5P and D-Xu5P. The finding of different CD spectra in the near-UV region of both the substrate and product made possible the measurement of kinetic deuterium isotope effects for the epimerization reaction by the equilibrium perturbation method. Figure 5 shows that there is a shift toward higher ellipticity of L-Ru5P from pH 5.5 to 7.0. The trend is reversed for D-Xu5P, but the magnitude of the shift is smaller. CD spectra of L-Ru5P at each pH but without a buffer produced the same results, showing that the ellipticity dependence on pH is not due to a "buffer effect". The source of the CD signal is the n−π^*

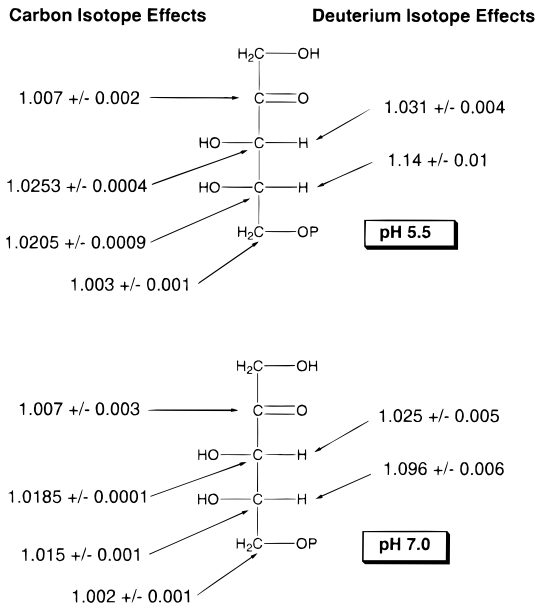

FIGURE 6: ^{13}C and deuterium kinetic isotope effects from wild-type L-Ru5P 4-epimerase at pH 5.5 and 7.0. Data were collected with Zn^{2+} 4-epimerase. See Experimental Procedures for experimental conditions.

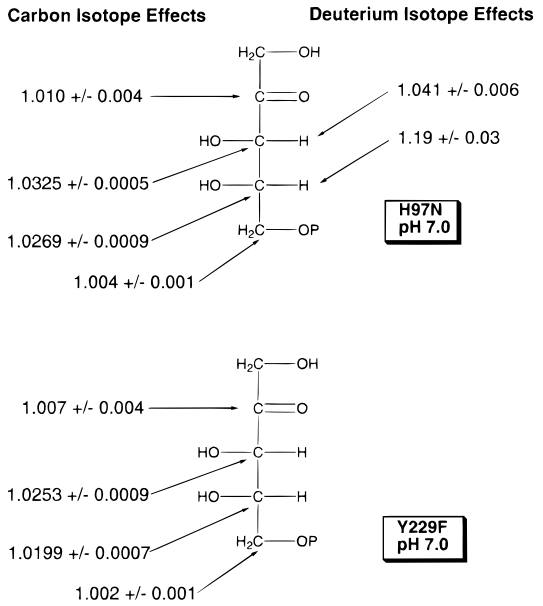

FIGURE 7: ^{13}C and deuterium kinetic isotope effects from Y229F and H97N mutants at pH 7.0. Data were collected with Zn^{2+} mutant 4-epimerases. See Experimental Procedures for experimental conditions.

electronic transition of the carbonyl group (*39*). The absorption spectra of both L-Ru5P and D-Xu5P exhibit absorption maxima centered around the CD peaks, but the signals are relatively weak (not shown).

^{13}C Kinetic Isotope Effects. All isotope effect measurements were carried out with Zn(II)-substituted wild-type and mutant 4-epimerases. The ^{13}C isotope effects of the epimerization reaction were measured with the wild-type 4-epimerase at pH 5.5 and 7.0 (Figure 6), the Y229F mutant at pH 7.0 (Figure 7), and the H97N mutant at pH 7.0 (Figure 7). For the wild-type 4-epimerase, the ^{13}C kinetic isotope effects exhibited smaller values at pH 7.0 than at pH 5.5. The ^{13}C isotope effects for Y229F at pH 7.0 were essentially the same as those for the wild-type enzyme at pH 5.5. The ^{13}C isotope effects for H97N at pH 7.0 were the largest.

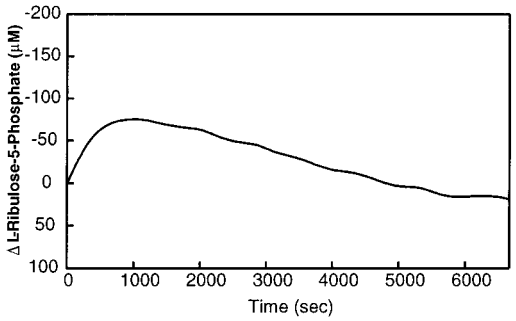

FIGURE 8: Deuterium kinetic isotope effect measured by equilibrium perturbation with 8.79 mM L-Ru5P and 16.7 mM D-[3-^{2}H]Xu5P and the H97N mutant at pH 7.0.

Deuterium Kinetic Isotope Effects from D-[3-^{2}H]Xu5P and D-[4-^{2}H]Xu5P by Equilibrium Perturbation. All isotope effect measurements were carried out with Zn(II)-substituted wild-type and mutant 4-epimerases. The equilibrium constants that were measured from the undeuterated (L-Ru5P) and deuterated (D-[3-^{2}H]Xu5P and D-[4-^{2}H]Xu5P) substrates resulted in values close to 1.90. Thus, as expected the equilibrium deuterium isotope effects at C-3 and C-4 were unity. The deuterium kinetic isotope effects were calculated from the measured equilibrium perturbations for the wild-type 4-epimerase at pH 7.0 and 5.5 (Figure 6) and the H97N mutant at pH 7.0 (Figure 7). As was the case for the ^{13}C isotope effects, the measured deuterium isotope effect for the wild-type enzyme exhibited larger values at pH 5.5 than at pH 7.0. The H97N exhibited the largest values. The deuterium kinetic isotope effects were not measured for the Y229F mutant because the enzyme had very low activity (*24*) and the use of large quantities of Y229F in the cuvette created a great deal of noise in the data collection. An example of an equilibrium perturbation measurement for the L-Ru5P/D-[3-^{2}H]Xu5P mixture is shown in Figure 8.

DISCUSSION

The sequence alignments of L-Ru5P 4-epimerase, L-Fuc1P aldolase, and L-Rhu1P aldolase (Figure 2), particularly the alignment with the residues of L-Fuc1P aldolase that are involved in metal ion and phosphate binding (*21*−*23*), suggest that these three enzymes are evolutionally related. Additionally, the findings by Wood and co-workers that the 4-epimerase has no requirement for pyridine dinucleotides for activity (*13*, *14*), has an absolute requirement for divalent metal cations (*15*), and does not catalyze exchange with solvent during the epimerization reaction (*14*, *16*) suggest that the L-Ru5P 4-epimerase has a novel catalytic mechanism. Deupree and Wood (*15*) proposed two possible mechanisms that may explain the catalytic processes involved in the epimerization reaction (Figure 1). In conjunction with the information previously collected and the finding of sequence alignments between the 4-epimerase and the aldolases, we wished to determine whether the 4-epimerase catalyzes the epimerization reaction via the aldol cleavage−condensation mechanism or the dehydration−hydration mechanism or by a catalytic process involving a mechanism previously unforeseen.

If the epimerization reaction occurs by the aldol cleavage−condensation mechanism (Figure 1A), one would expect to find primary ^{13}C isotope effects at C-3 and C-4, and possibly a secondary ^{13}C isotope effect at C-2, and one would expect to find secondary deuterium isotope effects at C-3 and C-4. If the reaction occurs by the dehydration−hydration mechanism (Figure 1B), one would expect to find similar ^{13}C isotope effects. However, there would be a primary deuterium isotope effect at C-3 and a secondary effect at C-4.

Maximum primary deuterium kinetic isotope effects can be as large as 7−10 (*40*), while secondary deuterium kinetic isotope effects are much smaller, typically ≤1.4 (*40*). Hence, the difference between primary and secondary deuterium kinetic isotope effects is clearly discernible. If the epimerization reaction occurs by the aldol cleavage−condensation mechanism, the expected maximum secondary deuterium kinetic isotope effects, as calculated from fractionation factors (*34*), are 1.20 (or 20%) at C-3 and 1.40 (or 40%) at C-4. These calculations are based on the change in hybridization at C-3 and C-4 from sp^3 to sp^2 for the C−C bond cleavage reaction. If the reaction occurs by the dehydration−hydration mechanism, the theoretical limit for the secondary deuterium kinetic isotope effect at C-4 is expected to be 1.33 (or 33%). Again, the calculation is based on the change in the extent of hybridization at C-4 from the hydroxyl group elimination reaction. Although it would be difficult to calculate the primary deuterium kinetic isotope effect at C-3 for the dehydration−hydration mechanism, the value is expected to be large and would certainly be distinguishable from a secondary isotope effect.

For the wild-type 4-epimerase at pH 5.5 (Figure 6), the deuterium isotope effects at C-3 (3.1%) and C-4 (14%) are very small and in the range of secondary deuterium isotope effects. However, there is a possibility that commitments to catalysis are suppressing the intrinsic isotope effects to produce the appearance of a small secondary deuterium isotope effect at C-3 (*29*). This possibility is eliminated since one observes a sizable carbon isotope effect of 2.53% at C-3. Since the theoretical maximum of a primary ^{13}C kinetic isotope effect is ∼5% (*40*), a value of 2.53% indicates that the intrinsic isotope effect is not greatly reduced by commitments to catalysis and thus the observed deuterium isotope effect of 3.1% must be a secondary effect. The results therefore are highly supportive of the aldol cleavage−condensation mechanism for the epimerization reaction (Figure 1A).

As expected from the pH profile (Figure 4), the ^{13}C kinetic isotope effects for wild-type 4-epimerase at C-3 and C-4 are smaller at pH 7.0, the maximum point of the *V*/*K* profile and the location with the greatest commitments to catalysis (*29*, *41*). At pH 5.5, where the *V*/*K* value is small and the commitments to catalysis are smallest, the ^{13}C kinetic isotope effects are larger (*29*, *41*). The k_{cat} value for the wild-type 4-epimerase is 10.6 s^{-1} at pH 7.0 and 4.23 s^{-1} at pH 5.5. The Y229F mutant, on the other hand, is more than 3 orders of magnitude less active than the wild-type 4-epimerase (*24*) and yet exhibits the same ^{13}C kinetic isotope effect values at pH 7.0, within experimental error, as the wild-type enzyme at pH 5.5 (Figure 7). The H97N mutant has almost one-tenth the activity of the wild-type enzyme (*24*) and exhibits the largest isotope effect values at pH 7.0 (Figure 7). One can conclude from the ^{13}C isotope effects that the wild-type enzyme has no external commitment to catalysis at pH 5.5, while at pH 7, it has both internal and external commitments (see below). The mutation at Tyr229 has eliminated the external commitment for the 4-epimerase, and the commitments for the H97N mutant are probably completely eliminated. The chemistry of the catalyzed epimerization reaction by the H97N mutant is entirely, or almost entirely, rate-limiting. Therefore, both the measured ^{13}C and deuterium isotope effects for the H97N mutant represent intrinsic isotope effect values.

A small secondary ^{13}C isotope effect is seen at C-2, probably resulting from the loss of bending or torsional modes during the cleavage reaction. The secondary ^{13}C isotope effect at C-5 is still smaller, and presumably results from the same cause.

Since secondary kinetic isotope effects are thought to show the simplest dependence on transition state structure, a secondary deuterium kinetic isotope effect of 19% at C-4 for the H97N mutant, about half of the predicted 40%, would suggest that the transition state for the C−C bond cleavage of the epimerization reaction lies midway between the reactant state and the intermediate state of the reaction. Interestingly, the secondary deuterium kinetic isotope effect at C-3 (4.1%) is only one-fifth of the predicted value. The reason for this difference is that the calculated values of the secondary isotope effects are derived from fractionation factors of molecules that are in aqueous solution and *not* enzyme-bound. The binding of the oxygen atoms on C-2 and C-3 of L-Ru5P to the zinc center in the cis conformation would cause the C−H bond at C-3 to be nearly in the $O-C_2-C_3-O$ plane, since C-4 must be in the out-of-plane position for cleavage to occur. This would result in a significant decrease in the extent of hyperconjugation between the C−H bond and the adjacent carbonyl group relative to what occurs in solution, and would cause an increase in the fractionation factor of the hydrogen nucleus at C-3. We estimate that the fractionation factor of the hydrogen at C-3 of L-Ru5P is 1.10 in solution, but 1.16 if hyperconjugation is prevented, while the fractionation factor of the hydrogen in the enediolate is 0.92 (*34*). The observed secondary deuterium isotope effect of 1.041 suggests a fractionation factor in the transition state of 1.06, which is one-third of the way from a value of 1.16 to one of 0.92.

To analyze the catalytic mechanism of the 4-epimerase further, the reaction can be written

$$E \underset{k_2}{\overset{k_1S}{\rightleftharpoons}} ES \underset{k_4}{\overset{k_3}{\rightleftharpoons}} ES^* \underset{k_6}{\overset{k_5}{\rightleftharpoons}} EI_1^* \underset{k_8}{\overset{k_7}{\rightleftharpoons}} EI_2^* \underset{k_{10}}{\overset{k_9}{\rightleftharpoons}} EP^* \underset{k_{12}}{\overset{k_{11}}{\rightleftharpoons}} EP \xrightarrow{k_{13}} E + P \quad (9)$$

where ES represents the enzyme−substrate complex, ES* the activated substrate complex, EI_1* the enediolate−glycolaldehyde phosphate complex, EI_2* the intermediate complex with the C−C bond of glycolaldehyde phosphate rotated 180°, EP* the activated product complex after the bond between C-3 and C-4 has regenerated, EP the enzyme−product complex, and E the free Zn(II) 4-epimerase. k_5, k_6, k_9, and k_{10} are for steps that are isotopically sensitive to both ^{13}C and deuterium substitution, while the other steps,

including k_7 and k_8 for bond rotation or molecular motion, are not.

The equation for the observed ^{13}C kinetic isotope effect, $^{13}(V/K)$, for mechanism 9 at C-2−C-4 can be derived as

$$^{13}(V/K) = \frac{^{13}K_{eq5}\,^{13}k_9 + {}^{13}k_5\frac{k_7k_9}{k_8k_6} + \frac{k_7k_9}{k_8k_6}C_f + {}^{13}K_{eq5}\frac{k_9}{k_8} + {}^{13}K_{eq5}\,^{13}K_{eq9}C_r}{1 + \frac{k_7k_9}{k_8k_6} + \frac{k_7k_9}{k_8k_6}C_f + \frac{k_9}{k_8} + C_r} \quad (10)$$

$$C_f = \frac{k_5}{k_4}\left(\frac{k_2 + k_3}{k_2}\right) \quad C_r = \frac{k_{10}}{k_{11}}\left(\frac{k_{12} + k_{13}}{k_{13}}\right) \quad (11)$$

$$^{13}K_{eq5} = \frac{^{13}k_5}{^{13}k_6} \quad ^{13}K_{eq9} = \frac{^{13}k_9}{^{13}k_{10}} \quad (12)$$

where $^{13}k_5$, $^{13}k_6$, $^{13}k_9$, and $^{13}k_{10}$ are the intrinsic carbon isotope effects for the isotopically sensitive steps. The observed secondary deuterium kinetic isotope effects at C-3 and C-4, $^{D}(V/K)$, for mechanism 9 are also given by eqs 10−12 with the superscript 13 replaced by D. Therefore, the discussion of the carbon isotope effects can be applied without modification for the deuterium kinetic isotope effects. $^{13}K_{eq5}$ and $^{13}K_{eq9}$ are the first and second ^{13}C equilibrium isotope effects for the two isotopically sensitive steps, k_5 and k_9. The product of the two equilibrium isotope effect expressions represents the ^{13}C equilibrium isotope effect for the overall epimerization reaction, $^{13}K_{eq}$, which is unity.

Equation 10 can be further simplified if some assumptions are made. Since the catalyzed reaction is an epimerization reaction with K_{eq} being equal 1.9, there are pairs of reactive species that are nearly equivalent in free energy. L-Ru5P and D-Xu5P are nearly equivalent, as are their activated complexes, and so are the two intermediate states where the difference is in the rotation of the C−C bond of the glycolaldehyde phosphate fragment. Therefore, k_9/k_6 and k_7/k_8 are both approximately 1. The isotope effects on isotopically sensitive steps $^{13}k_6$ and $^{13}k_9$ are equal, and those of $^{13}k_5$ and $^{13}k_{10}$ are equal. This causes the expression $^{13}K_{eq5}\,^{13}k_9$ to reduce to $^{13}k_5$ and $^{13}K_{eq5}\,^{13}K_{eq9}$ to become 1. Equation 10 can thus be rewritten as

$$^{13}(V/K) = \frac{2\,^{13}k_5 + C_f + {}^{13}K_{eq5}\frac{k_9}{k_8} + C_r}{2 + C_f + \frac{k_9}{k_8} + C_r} \quad (13)$$

where $^{13}K_{eq5}$, C_f, and C_r remain the same as in eqs 11 and 12. Since C_f and C_r occur as the sum in both numerator and denominator, they can simply be replaced by C.

For the H97N mutant, eq 13 can be further simplified since it is believed that this mutant has little or no commitment to catalysis, on the basis of the finding that the ^{13}C isotope effects at C-3 and C-4 are very large compared to those of the wild-type enzyme and the Y229F mutant. Equation 13 can be rewritten to represent the observed isotope effects from the H97N mutant as

$$^{13}(V/K) = \frac{^{13}k_5 + {}^{13}K_{eq5}\frac{k_9}{2k_8}}{1 + \frac{k_9}{2k_8}} \quad (14)$$

It is interesting to note at this point that the observed isotope effect for the H97N mutant is dependent on the k_9/k_8 ratio. If the rate of C−C bond rotation of the glycolaldehyde phosphate intermediate, k_8, is much faster than the rate of C−C bond formation between C-3 and C-4, k_9, eq 14 would reduce to $^{13}(V/K) = {}^{13}k_5$ and the observed isotope effect will consist predominantly of the intrinsic isotope effect from step k_5. If $k_9 > k_8$, eq 14 becomes $^{13}(V/K) = {}^{13}K_{eq5}$ and the observed isotope effect would be the equilibrium isotope effect for the C−C bond cleavage reaction. If $k_9 = k_8$, the observed kinetic isotope effect will be between the intrinsic isotope effect, $^{13}k_5$, and the equilibrium isotope effect, $^{13}K_{eq5}$.

Since it is reasoned from the secondary deuterium kinetic isotope effects of the H97N mutant that the transition state for C−C cleavage of L-Ru5P is midway between the ground state and the intermediate state, the observed isotope effects therefore should correspond closely to the intrinsic isotope effects. This suggests that $^{13}K_{eq5}$ makes very little contribution to the observed isotope effect for the H97N mutant and that the k_9/k_8 ratio must be very small. This is not surprising since C−C bond rotation has an energetic barrier of only 3 kcal/mol (*42*). Of course, the k_9/k_8 ratio may be different among the wild-type 4-epimerase, the Y299F mutant, and the H97N mutant, with the ratio possibly being smaller for the H97N mutant than for the wild-type enzyme or for the Y229F mutant. Therefore, the analysis above may be more appropriately applied to the H97N mutant than to the wild-type 4-epimerase or to the Y229F mutant.

However, if the same analysis is applied to both the wild-type 4-epimerase and the Y229F mutant, with the assumption that k_7 and k_8 are much greater than the rate of bond formation (k_6 and k_9), mechanism 9 reduces to mechanism 15 and eq 13 reduces to eq 16.

$$E \underset{k_2}{\overset{k_1S}{\rightleftharpoons}} ES \underset{k_4}{\overset{k_3}{\rightleftharpoons}} ES^* \underset{k_6}{\overset{k_5}{\rightleftharpoons}} EI^* \underset{k_{10}}{\overset{k_9}{\rightleftharpoons}} EP^* \underset{k_{12}}{\overset{k_{11}}{\rightleftharpoons}} EP \xrightarrow{k_{13}} E + P \quad (15)$$

$$^{13}(V/K) = \frac{2\,^{13}k_5 + C_f + C_r}{2 + C_f + C_r} \quad (16)$$

Note that the only difference between mechanisms 9 and 15 is the removal of steps k_7 and k_8. C_f and C_r are the same as in eq 11.

Since C_f and C_r occur as the sum in both numerator and denominator, eq 16 may thus be further simplified to

$$^{13}(V/K) = \frac{^{13}k_5 + C}{1 + C} \quad (17)$$

where C is the average of C_f or C_r in eq 11. Because commitments to catalysis are composed of an external and an internal component (*29*), C_f and C_r from eq 11 can be

Table 1: Calculation of Internal and External Commitments for the Wild-Type Enzyme at pH 5.5 and 7.0

	C_{ext}[a]	C_{int}[b]	C[c]
wild type at pH 7.0	1.18(1.67)	0.471(0.71)	1.65(2.38)
wild type at pH 5.5[d]	0(0)	0.471(0.71)	0.471(0.71)

[a] k_3/k_2 or k_{12}/k_{13} ratios can be calculated from both the C_{ext} and C_{int} values. See the text in the Discussion. [b] $C_{int} = k_5/k_4$ or k_{10}/k_{11}. [c] Total of C_{ext} and C_{int}. The first values represent calculations from ^{13}C isotope effect data at C-3. Values in parentheses are from C-4 data. [d] The commitments for the Y229F mutant at either pH 5.5 or 7.0 are the same as for the wild type at pH 5.5. The H97N mutant has no internal or external commitments.

re-expressed as

$$C_f = \frac{k_5 k_3}{k_4 k_2} + \frac{k_5}{k_4} = C_{f-ext} + C_{f-int} \quad (18)$$

$$C_r = \frac{k_{10} k_{12}}{k_{11} k_{13}} + \frac{k_{10}}{k_{11}} = C_{r-ext} + C_{r-int} \quad (19)$$

C_{ext}, the external component of commitment to catalysis, is pH-dependent, while C_{int}, the internal component, is not (*29*).

Since the mutation at Tyr229 is believed to eliminate the external commitments and the mutation at His97 is believed to have removed all commitments to catalysis, eqs 17−19 can be used with the ^{13}C kinetic isotope effect data from the wild-type enzyme and the two mutants to calculate both the external and internal commitments to catalysis for all three enzymes. Table 1 is a tabulation of the results from these calculations.

As Table 1 shows, the calculations were made from the ^{13}C kinetic isotope effects at C-3 and C-4 of L-Ru5P. The commitment values are slightly different but can be averaged to simplify the discussion. As the calculations show, the external commitments are more than twice the magnitude of the internal commitments. Calculation of the k_3/k_2 ratio gives an average value of 2.4, while the k_5/k_4 ratio has an average value of 0.59. The k_3/k_2 ratio shows that once the substrate is bound to the enzyme it is 2.4 times more likely to proceed toward the activated complex than to be released to the aqueous solvent. The k_5/k_4 ratio indicates that once the substrate has approached the status of an activated complex, it has about a 30% chance to proceed toward the C−C bond cleavage step as opposed to reverting back to the unactivated complex.

The ^{13}C and deuterium kinetic isotope effects show that the 4-epimerase catalyzed L-Ru5P to D-Xu5P epimerization proceeds by the aldol cleavage−condensation mechanism (Figure 1A). The L-Ru5P 4-epimerase is thus a unique epimerase that catalyzes an epimerization reaction via a mechanism that is unlike other previously characterized epimerases. The finding of sequence alignment between the 4-epimerase with L-Fuc1P aldolase and L-Rhu1P aldolase suggests that the 4-epimerase and the two aldolases are evolutionally related. Recently, Johnson and Tanner reported that L-Ru5P 4-epimerase catalyzes a slow aldol condensation reaction between dihydroxyacetone and glycolaldehyde phosphate and that during the epimerization reaction of L-Ru5P and D-Xu5P some leakage of the intermediates was detected (*20*). Our work supports the characterization of L-Ru5P 4-epimerase as a "masked aldolase" (*20*).

ACKNOWLEDGMENT

We thank Dr. Nancy Lee of the University of California at Santa Barbara for her generous gift of the pNL16 plasmid and the *E. coli* B/r D^{-139} strain and Dr. Darrell McCaslin of the University of Wisconsin−Madison Biophysics Instrumentation Facility for his helpful suggestions and comments on the CD spectroscopy portion of this paper.

SUPPORTING INFORMATION AVAILABLE

Detailed description of overexpression and purification of ribulokinase and L-ribulose-5-phosphate epimerase. This material is available free of charge via the Internet at http://pubs.acs.org.

REFERENCES

1. Englesberg, E., Anderson, R. L., Weinberg, R., Lee, N., Hoffee, P., Huttenhauer, G., and Boyer, H. (1962) *J. Bacteriol. 84*, 137−146.
2. Lee, N., Gielow, W., Hamilton, E., and Fowler, A. (1986) *Gene 47*, 231−244.
3. Shieh, W. R., and Chen, C. S. (1993) *J. Biol. Chem. 268*, 3487−3493.
4. Gelb, M. H., Lin, Y., Pickard, M. A., Song, Y., and Vederas, J. C. (1990) *J. Am. Chem. Soc. 112*, 4932−4942.
5. Ramaswamy, S. G. (1984) *J. Biol. Chem. 259*, 249−254.
6. Fuller, J. G., and Leadlay, P. F. (1983) *Biochem. J. 213*, 643−650.
7. Ding, L., Seto, B. L., Ahmed, A. S., and Coleman, W. G. (1994) *J. Biol. Chem. 269*, 24384−24390.
8. Burke, J. R., and Frey, P. A. (1993) *Biochemistry 32*, 13220−13230.
9. Glaser, L. (1972) in *The Enzymes* (Boyer, P. D., Ed.) Vol. 6, pp 355−380, Academic Press, New York.
10. Hucho, F., and Wallenfels, K. (1971) *Eur. J. Biochem. 23*, 489−496.
11. Chance, E. M., Hess, B., Plesser, T., and Wurster, B. (1975) *Eur. J. Biochem. 50*, 419−424.
12. Shirokane, Y., and Suzuki, M. (1995) *FEBS Lett. 367*, 177−179.
13. Deupree, J. D., and Wood, W. A. (1970) *J. Biol. Chem. 245*, 3988−3995.
14. McDonough, M. W., and Wood, W. A. (1961) *J. Biol. Chem. 236*, 1220−1224.
15. Deupree, J. D., and Wood, W. A. (1972) *J. Biol. Chem. 247*, 3093−3097.
16. Davis, L., Lee, N., and Glaser, L. (1972) *J. Biol. Chem. 247*, 5862−5866.
17. Salo, W. L., Fossitt, D. D., Bevill, R. D., Kirkwood, S., and Wood, W. A. (1972) *J. Biol. Chem. 247*, 3098−3100.
18. Hoerecker, B. L., Tsolas, O., and Lai, C. Y. (1972) in *The Enzymes* (Boyer, P. D., Ed.) Vol. 7, pp 213−258, Academic Press, New York.
19. Malmstrom, B. G. (1961) in *The Enzymes* (Boyer, P. D., Lardy, H., and Myrback, K., Eds.) Vol. 5, pp 455−469, Academic Press, New York.
20. Johnson, A. E., and Tanner, M. E. (1998) *Biochemistry 37*, 5746−5754.
21. Dreyer, M. K., and Schulz, G. E. (1993) *J. Mol. Biol. 231*, 549−553.
22. Dreyer, M. K., and Schulz, G. E. (1996) *Acta Crystallogr. D52*, 1082−1091.
23. Dreyer, M. K., and Schulz, G. E. (1996) *J. Mol. Biol. 259*, 458−466.
24. Lee, L. V., Poyner, R. R., Vu, M. V., and Cleland, W. W. (2000) *Biochemistry 39*, 4821−4830.
25. Lee, N., and Bendet, I. (1967) *J. Biol. Chem. 242*, 2043−2050.
26. Lee, N., Patrick, J. W., and Masson, M. (1968) *J. Biol. Chem. 243*, 4700−4705.

27. Anderson, R. L. (1966) *Methods Enzymol. 9*, 48−51.
28. Cleland, W. W. (1967) *Adv. Enzymol. 29*, 1−32.
29. Cleland, W. W. (1982) *CRC Crit. Rev. Biochem. 13*, 385−427.
30. Racker, E. (1961) in *The Enzymes* (Boyer, P. D., Lardy, H., and Myrback, K., Eds.) Vol. 5, pp 397−412, Academic Press, New York.
31. Canellas, P. F., and Cleland, W. W. (1991) *Biochemistry 30*, 8871−8876.
32. Janson, C. A., and Cleland, W. W. (1974) *J. Biol. Chem. 249*, 2562−2566.
33. Walsh, C. (1979) *Enzymatic Reaction Mechanism*, W. H. Freeman and Co., New York.
34. Cleland, W. W. (1980) *Methods Enzymol. 64*, 104−125.
35. Cleland, W. W. (1977) in *Isotope Effects on Enzyme-Catalyzed Reactions* (Cleland, W. W., O'Leary, M. H., and Northrop, D. B., Eds.) pp 153−175, University Park Press, Baltimore.
36. Lu, Z., and Lin, E. C. C. (1989) *Nucleic Acids Res. 17*, 4883−4884.
37. Genetics Computer Group (1999) *Wisconsin Package*, version 10.0, Madison, WI.
38. Moralejo, P., Egan, S. M., Hidalgo, E., and Aguilar, J. (1993) *J. Bacteriol. 175*, 5585−5594.
39. Bystricky, S., Sticzay, T., and Tvaroska, I. (1980) *Czech. Chem. Commun. 45*, 475−481.
40. Cook, P. F. (1991) *CRC Enzyme Mechanism from Isotope Effects*, CRC Press, Boca Raton, FL.
41. Northrop, D. B. (1977) in *Isotope Effects on Enzyme-Catalyzed Reactions* (Cleland, W. W., O'Leary, M. H., and Northrop, D. B., Eds.) pp 122−152, University Park Press, Baltimore.
42. Levine, I. N. (1988) *Physical Chemistry*, 3rd ed., McGraw-Hill, New York.

BI992894+